JOURNAL OF PROPULSION AND POWER
Vol. 21, No. 5, September–October 2005

Effect of Magnetohydrodynamics Interaction in Various Parts of Diffuser on Inlet Shocks: Experiment

S. V. Bobashev,* A. V. Erofeev,† T. A. Lapushkina,‡ S. A. Poniaev,§ and R. V. Vasil'eva†
Ioffe Physico-Technical Institute Russian Academy of Sciences, 194021, St. Petersburg, Russia
and
D. M. Van Wie¶
Johns Hopkins University, Applied Physics Laboratory, Laurel, Maryland 20723

The effects of external magnetic and electric fields on the position of attached shocks in a supersonic diffuser were studied. Experiments were conducted at a Mach number at the diffuser inlet of $M = 4.3$. The working gas was Xe plasma, formed using a reflected shock tube with an accelerating convergent-divergent nozzle. Magnetohydrodynamic experiments with an external transverse electric field in the decelerating and accelerating regimes and experiments with a longitudinal electric field were carried out. The interaction of the flow with the external fields in different parts of the diffuser was achieved by circulating current through different segmented electrodes. It has been found that application of external fields near the inlet leading edge is the most efficient.

Nomenclature

A	=	work generated by Lorentz force
B	=	magnetic induction
F	=	Lorentz force
h	=	duct width
I	=	current
j	=	current density
k	=	load coefficient
L	=	interaction zone length
M	=	Mach number
N	=	magnetohydrodynamic interaction parameter (Stuart number)
q	=	thermal energy
R_{eff}	=	effective resistance of plasma
R_L	=	load resistance
u	=	flow velocity
V	=	voltage
x_c	=	axial position of shock crossing
α	=	angle between attached shocks
β	=	Hall parameter
ν_e	=	electron/heavy-particle collision frequency
ρ	=	gas density
φ	=	angle between diffuser wall and attached shock
ω_e	=	electron cyclotron frequency

Introduction

At present, great attention is paid to different methods for control of hypersonic flight vehicles.[1] This paper describes experimental studies investigating the possibility of controlling inlet shocks in a hypersonic diffuser by magnetohydrodynamic (MHD) methods at flight Mach numbers of 4–8. This problem was initiated by the "AJAX" concept[1,2] and was further developed in a number of works.[3–10]

At the Mach numbers between 4 and 8, thermal ionization of air behind a shock wave is insufficient to give rise to any considerable electrical conductivity, and so different methods of air ionization involving the use of external ionizers are being developed.[7] Such methods should ensure a conductivity sufficient for the MHD interaction ($\sigma = 10$–100 S/m), and the energy required for ionization should not be more than several percent of the electric power generated by an airborne MHD generator.

At present, the problem of air ionization in the inlet is far from solved; however, some gasdynamic aspects of the interaction of a supersonic flow with magnetic and electric fields can be addressed in experiments using an ionized inert gas flow.[11–17] The advantage of an inert gas plasma is that the characteristic time of recombination of charged particles is several orders of magnitude longer than the characteristic time of electron loss in an air plasma.[18,19] This leads to conservation of the initial ionization during a relatively long period of time. Such an ionized gas flow can be formed, for example, in a shock tube with a convergent-divergent nozzle.[11] Note that when the ionized inert gas flow is affected by magnetic and electric fields, a significant selective heating of electrons occurs that supports and enhances the initial ionization.[20,21]

In gasdynamic problems (in particular, MHD problems[22]), the main distinction between air and inert gas consists in different values of their isentropic exponents $\gamma = C_p/C_v$; therefore, the flow modeling does not involve this parameter. The flow is modeled via the main criteria of plasma flow interaction with the magnetic and electric fields. These are the Mach number of the flow M, the MHD interaction parameter (also called the Stuart number) $N = jBL/(\rho u^2)$, parameter of action of an external electric field $Q = jEL/u$, the Hall parameter $\beta = \omega_e/\nu_e$, and load coefficient $k = R_L/(R_L + R_{\text{eff}})$.

The results obtained in experiments with inert gases can be used for validating the numerical models. Then these models can be used for calculation of flows of gases with different values of γ. The calculations for the conditions of the experiment presented here are described in Refs. 8–10.

The main goal of this work was to find the most efficient methods of external control of attached shocks in a diffuser. To this end, the effects of external fields on attached shocks for different directions of the Lorentz force and also for localization of external effects in different parts of the diffuser were studied. For MHD interactions in the small models investigated, an external electric field had to be applied to compensate for a large near-electrode potential drop revealed in earlier studies of current-voltage characteristics.[12–15]

Presented as Paper 2002-5183 at the AIAA/AAAF 11th International Conference Space Planes and Hypersonic Systems and Technologies, Orleans, France, 29 September 2002; received 23 May 2003; revision received 20 September 2004; accepted for publication 24 October 2004. Copyright © 2005 by the authors. Published by the American Institute of Aeronautics and Astronautics, Inc., with permission. Copies of this paper may be made for personal or internal use, on condition that the copier pay the $10.00 per-copy fee to the Copyright Clearance Center, Inc., 222 Rosewood Drive, Danvers, MA 01923; include the code 0748-4658/05 $10.00 in correspondence with the CCC.

*Professor; s.bobashev@mail.ioffe.ru. Member AIAA.
†Senior Scientist; alex.erofeev@mail.ioffe.ru.
‡Scientist; tanyusha@mail.ioffe.ru.
§Junior Scientist; serguei.poniaev@mail.ioffe.ru. Member AIAA.
¶Principal Staff Engineer; dave.wanvie@jhuapl.edu. Senior Member AIAA.

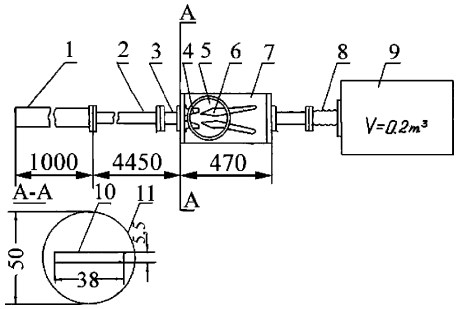

Fig. 1 Experimental setup: 1, high-pressure chamber; 2, low-pressure chamber; 3, measuring section of the low-pressure chamber; 4, flat nozzle; 5, optical window; 6, diffuser; 7, vacuum chamber; 8, sylphon; 9, exhaust tank; 10, cross section of the nozzle input; 11, shock-tube cross section. All dimensions are in millimeters.

Thus, the hypersonic gas flow was affected by both the MHD interaction and Joule gas heating in the external electric field. The latter resulted in deceleration of the supersonic flow. The MHD interaction could either accelerate or decelerate the flow.

Experiment

The experimental setup (Fig. 1) used a one-diaphragm shock tube including a high-pressure chamber for hydrogen with pressures up to 21 atm and a 4.5-m long low-pressure chamber filled with a heavy inert gas having a pressure of 30 mm Hg. At the end of the low-pressure chamber, there was a flat reflecting nozzle separated from the low-pressure chamber by a thin plastic (polyethylene terephthalate) diaphragm. The gas flow accelerated in the nozzle entered the diffuser, which had electrodes on its upped and lower surfaces. The nozzle and diffuser were placed in a vacuum chamber. A detailed description of the setup was given elsewhere.[12,13]

A pulsed magnetic field of up to 1.5 T (transverse to the flow) was generated by the discharge of a capacitor bank through coaxial Helmholtz coils situated on the sides of the vacuum chamber. An electric field of required magnitude and duration was produced by the discharge of a "long line" (a multicell LC circuit). In the experiment, the current density j distribution along the diffuser was measured. Near the diffuser leading edge the potential distribution between electrodes was measured, and the bulk σ_0 and effective conductivities were inferred.[16] To visualize the flow, an optical Schlieren system was developed.[11–16] Frame-by-frame filming was performed by a high-speed VSK-5 camera; a Podmoshenskii light source was used; the exposure time was 2.7 μs. A higher time resolution (30 ns) was obtained in the case of one-shot filming when a Q-switched OGM-20 laser was used as the light source.

The experiments were conducted in Xe at an incident shock Mach number of 8 and initial gas pressure in the low-pressure chamber of 30 torr. The calculated flow parameters at the diffuser inlet were Mach number $M = 4.3$; density $\rho = 0.127$ kg/m^3, flow velocity $u = 1.55 \times 10^3$ m/s; and conductivity $\sigma = 600$ mho/m. The test time was about 500 μs, and the magnetic field induction $B = 1.3$ T. The voltage applied to electrodes was varied between 100 and 400 V.

Types of Current Commutation

In the experiments, two types of current commutation were used. The first was the transverse current commutation (Fig. 2). In this commutation regime, current was circulated through electrode pairs placed on opposite diffuser walls.

The diffuser operates as a Faraday MHD channel with segmented electrodes. Owing to the segmented electrodes, the flow interaction with the external field could be achieved in different parts of the diffuser depending on which electrodes are used. In the channel, the electromotive force (EMF) was induced ($\varepsilon = uBh$, where h is the distance between paired electrodes). A voltage V from separate external sources was applied to electrodes. If the magnetically induced EMF and external electric field have the same direction, as shown in Fig. 2a, the regime is referred to as decelerating. When the EMF and external electric field are oppositely directed (Fig. 2b),

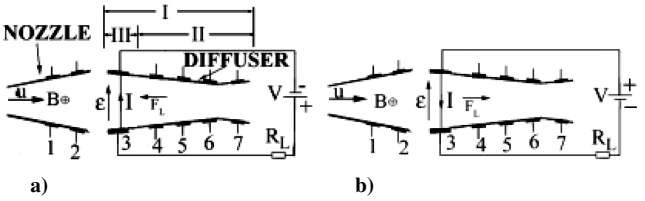

Fig. 2 Transverse current commutation: a) decelerating regime and b) accelerating regime, in which 1–7 are the number of electrodes, and the arrows show directions of current flow (I), EMF (ε), and Lorentz force (FL). I, II, and III are interaction regions: I, interaction in the whole diffuser volume; II, interaction in the entire diffuser volume with the exception of the leading-edge portion; III, interaction at the leading edge.

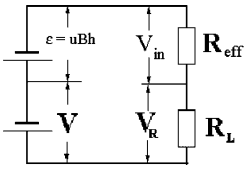

Fig. 3 Equivalent electric scheme.

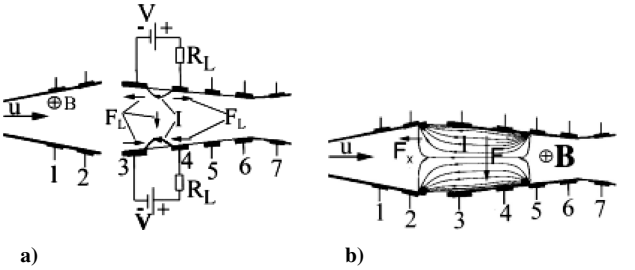

Fig. 4 Longitudinal current flow. The arrows show directions of flow velocity (u), current (I), magnetic field (B), and Lorentz force (F).

the regime is conditionally accelerating. Ohm's law in this case is given by

$$I R_{\text{eff}} = (1 - k)(uBh \pm V) \tag{1}$$

$$k = R_L/(R_L + R_{\text{eff}}) \tag{2}$$

where R_{eff} is the effective internal resistance of the gap between opposite electrodes. In out experiments, $R_L = 0.1$ Ω. The sign + before V in Eq. (1) denotes MHD deceleration, and sign − denotes MHD acceleration. In Fig. 2a, the three interaction regions used for the experiments are marked. The equivalent electric scheme of the setup is shown in Fig. 3.

The analysis of the volt-ampere characteristics given in Refs. 15 and 17 has shown that the effective conductivity of the plasma is significantly lower than the calculated one caused by a large near-electrode potential drop. It has also been found that the near-electrode potential drop in the decelerating regime is significantly larger than in the accelerating one. The measurements of R_{eff} for all of the gaps between opposite electrodes in the diffuser in the absence of magnetic fields ($B = 0$) have shown that the values of R_{eff} are close to each other and are in the range 0.2–0.3 Ω, and hence the load coefficient $k = 0.33$–0.25. In the presence of the magnetic field in the decelerating regime, the load coefficient decreases as a result of the Hall effect to $k = 0.2$–0.15 for any pair of the electrodes in the diffuser. In the accelerating regime, the load coefficient was determined for the third pair of electrodes, $k = 0.3$.

The second type of current commutation was longitudinal. In this case current was circulated through electrodes placed on the same diffuser wall. Depending on through which pairs of electrodes the current flowed, either local interaction (Fig. 4a) or interaction in the entire diffuser volume occurred (Fig. 4b).

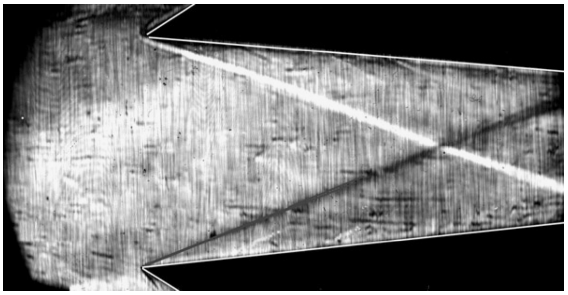

a)

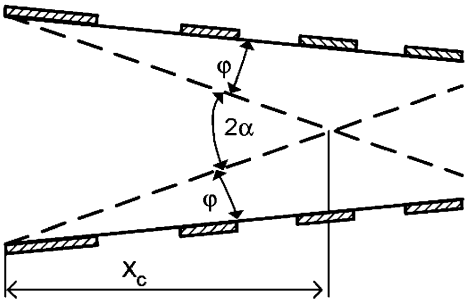

b)

Fig. 5 Schlieren picture of the flow in the absence of a) external fields and b) basic flow parameters.

Flow Pattern in the Absence of External Fields

To understand how attached shocks can be externally controlled, it is important to know how their positions can change in the diffuser under the action of external fields. Let us consider what parameters of the shock-wave structure can characterize the flow response to external fields. Figure 5a shows a schlieren picture of the flow in the diffuser obtained in the single-shot mode in the absence of external fields. It will be used as a reference picture for comparison with other shots. In the picture, the inlet shocks and their interactions are clearly seen.

Figure 5b shows the scheme of the shocks in the diffuser. The angle φ is the angle between the shock and diffuser wall. The attached shocks interact at an angle 2α at a distance x_c from the diffuser inlet. In the absence of external forces, $\varphi = 15$ deg, $x_c = 43$ mm, and $\alpha = 21.5$ deg.

All three parameters (φ, x_c, α) can be used as measures of external actions. In the case of flow deceleration, the Mach number decreases, and, as consequence, φ increases, distance x_c decreases, and angle α increases. In the case of flow acceleration, the changes in these parameters reverse.

Effect of External Fields on Different Diffuser Parts

The aim of this series of experiments was to find in what region of the diffuser the effect of external fields is most pronounced. The efficiency in this case implies attainment of a desired change in the shock-wave configuration at the lowest energy expenditure. The channel was operated as a MHD decelerator. Let us consider how the shock-wave configuration in the diffuser changes depending on which region of the diffuser the external fields are applied (Fig. 2).

Interaction Within the Whole Diffuser Volume (Region I)

Figure 6 shows schlieren pictures of the flow when the external voltage is applied to all pairs of electrodes in the diffuser (electrode pairs 3–7 in Fig. 2). Figure 6a shows the flow structure arising when only an external electric field is applied. The attached shocks, the shocks formed by reflection of attached shocks from each other, and the near-wall layer are clearly seen. Compared with the flow pattern in the absence of external fields (Fig. 5a), the angle of inclination of attached shocks is larger, the point of interaction of the shocks x_c is nearer to the diffuser inlet, and the sites of shock reflection from the wall are also closer to the diffuser inlet. Figure 6b shows a schlieren picture of the flow in the diffuser resulting from the combined action of electric and magnetic fields. It can be seen that the flow pattern differs much from that observed in the presence of the electric field alone. Of particular interest is the strongly developed near-wall layer, especially near the upper wall. The attached shocks have become more concave, and their point of interaction has moved closer to the diffuser inlet.

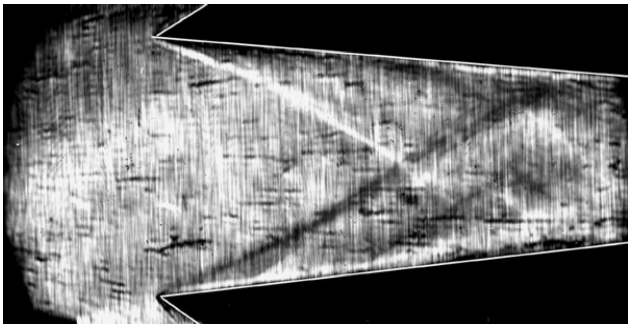

a) $V = 110$ V, $B = 0$

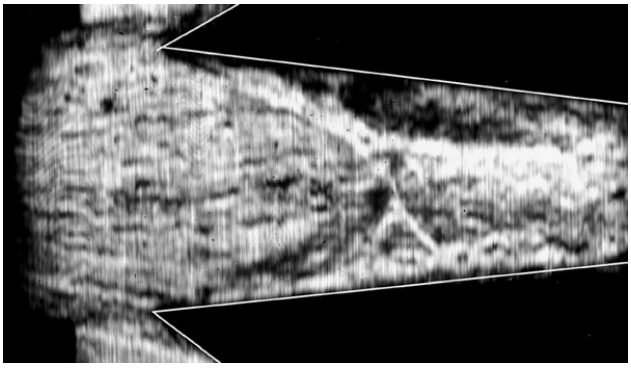

b) $V = 110$ V, $B = -1.3$ T

Fig. 6 Schlieren pictures of the flow in the case of interaction in the whole diffuser volume.

Interaction in Entire Diffuser Volume with Exception of Inlet Part (Region II)

Figure 7 shows the flow structure in the case when the external voltage is applied to all pairs of electrodes with the exception of the inlet leading edge (third) pair (electrodes 4–7 Fig. 2a). Figure 7a shows the flow structure arising when only the external electric field is applied. It can be seen from Fig. 7a that the angles of inclination of attached shocks differ only slightly from those shown in Fig. 5a; the distance x_c also remains the same. In this case the interaction with the external field leads to changes in positions of shock reflection from the wall (to be more exact, from the boundary layer). The shock reflections occur closer to the diffuser inlet. Figure 7b shows the shock-wave structure arising under a combined action of electric and magnetic fields. Because of a better adjustment of the schlieren system, more details are seen in Fig. 7b. It is evident that no considerable changes in the flow pattern have occurred.

Interaction at the Diffuser Inlet (Region III)

In the case when the external electric field is applied only to the third pair of electrodes placed at the diffuser inlet (see Fig. 2), the shock-wave configuration shown in Fig. 8 arises. If only the electric field is applied (Fig. 8a), a pronounced change in the angles of inclination of the shocks occurs, and the point of their interaction is closer to the diffuser inlet. MHD interaction (Fig. 8b) does not give rise to additional changes in x_c, but the attached shocks become concave, and wide near-wall layers are clearly seen. The upper layer (on the cathode wall) is much wider than the lower layer.

Table 1 Basic characteristics to external action

Region	L, m	$\langle j \rangle$, A/m^2	$\bar{N}$	$\bar{Q}$	Δx_c, mm
I	0.08 ± 0.001	$(7.0 \pm 0.35) \times 10^5$	0.52 ± 0.05	0.74 ± 0.07	8 ± 1
II	0.06 ± 0.001	$(7.0 \pm 0.35) \times 10^5$	0.39 ± 0.04	0.28 ± 0.03	0 ± 0.5
III	0.025 ± 0.001	$(4.0 \pm 0.2) \times 10^5$	0.09 ± 0.01	0.08 ± 0.008	7 ± 1

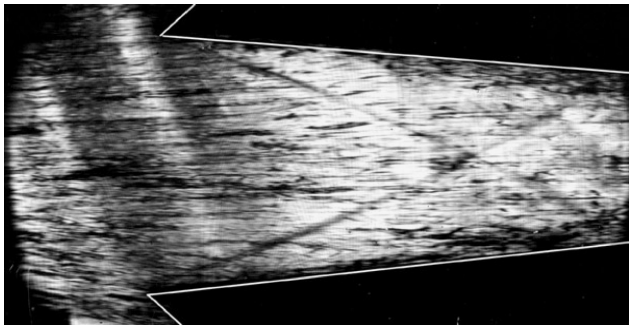

a) V = 110 V, B = 0

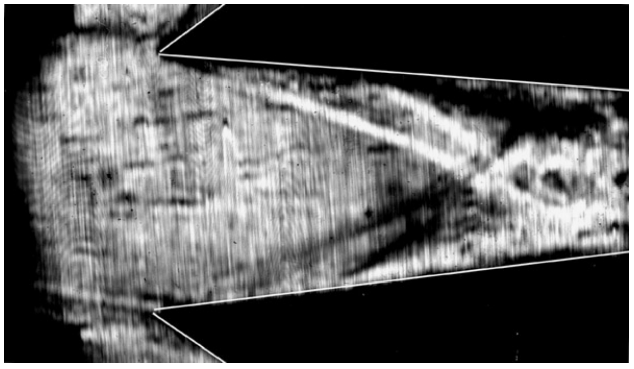

b) V = 110 V, B = −1.3 T

Fig. 7 Schlieren picture of the flow in the case of interaction in the entire diffuser volume with the exception of the inlet part.

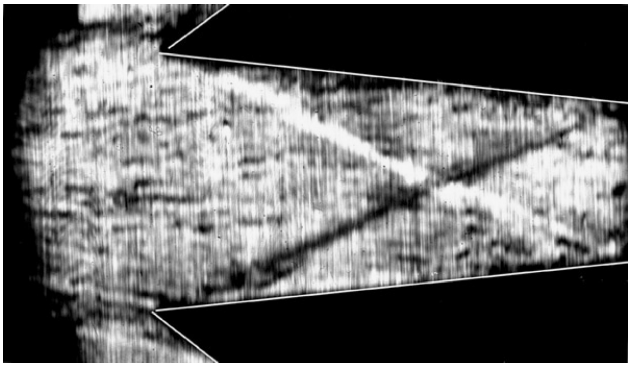

a) V = 110 V, B = 0

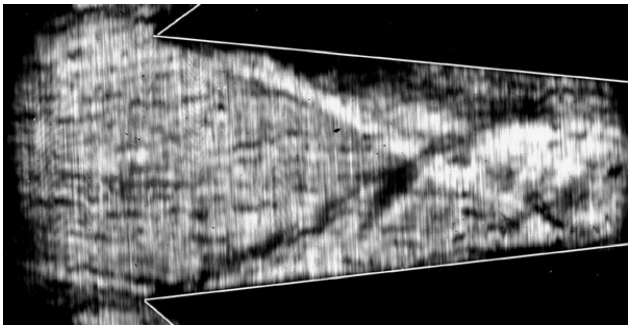

b) V = 110 V, B = −1.3 T

Fig. 8 Schlieren pictures of the flow in the case of interaction at the diffuser inlet.

Comparison of Effects of External Fields in Different Parts of Diffuser

Figures 5–9 show pictures of the flow under the influence of the external factors. Here, one can see the changes in the positions of the attached shocks and formation of new gasdynamic discontinuities and near-wall layers. The near-wall layers arise, first of all, as a result of a strong gas heating near the electrodes.[16] A detailed description of gasdynamic discontinuities and near-wall layers is given in Refs. 14 and 15. The main goal of the work described here was to see how the Lorentz force and Joule heating in different locations within the diffuser affect the positions of the attached shocks.

To compare quantitatively the energy needed to change the flow parameters for three interaction regions (I, II, and III, Fig. 2), we estimate the thermal energy q acquired by gas in the electric field and the work of the Lorentz force A. Because these parameters depend on current density, as shown by experiments,[12] the current density changes only slightly along the channel. The values of A and q are estimated as $A = \langle j \rangle BL$ and $q = \langle j \rangle^2 L/\sigma_0 \langle u \rangle$, where $\langle j \rangle$ is the measured current density averaged over the interaction region length, $\langle u \rangle$ is the calculated flow velocity averaged over the interaction region volume,[4,5] and $\sigma_0 = 250$ mho/m is the measured bulk conductivity.[16] We compare the energy of external factors with the kinetic flow energy $W = \langle \rho u^2 \rangle/2$ in the absence of external fields. W is averaged over the volume of the MHD interaction region with the help of theoretical data.[4,5] Thus, the basic characteristics of external action are defined by the dimensionless parameters: $\bar{N} = A/W$, and $\bar{Q} = q/W$. As a parameter characterizing changes in the shock-wave configuration, we take the change in the position of the interaction point of attached shocks $\Delta x_c = x_{c0} - x_c$, where x_{c0} is the position of the interaction point in the absence of external fields and x_c is the position of the interaction point in the presence of external fields. All basic characteristics, that is, interaction region length L, average current density $\langle j \rangle$, dimensionless parameters $\bar{N}$ and $\bar{Q}$, and values of Δx_c for different interaction regions, are listed in Table 1.

Let us compare the change in the shock-wave configurations occurring in the case of interaction in the inlet part of the diffuser (region III) and in the remaining part of the diffuser (region II). It is evident from Table 1 that the changes in positions of attached shocks in region II are much smaller than in region III in spite of a longer interaction length and higher energy of external actions per unit length in the former. Therefore, it can be concluded that it is more efficient to apply external fields to the diffuser inlet because in this case the most considerable changes in the shock-wave configuration occur at the lowest energy expenditure.

Decelerating and Accelerating Action of the Lorentz Force

Earlier experiments[12] revealed a strong effect of Joule heating on the flow structure. The aim of the experiment described here was to separate the actions of the Lorentz force and Joule heating. To demonstrate the flow acceleration and deceleration resulting from the action of the Lorentz force on the background of the decelerating action of Joule heating in the external electric field, we take three regimes with the same magnitude of current $|\mathrm{I}| = (500 \pm 50)$ A, but different directions of the Lorentz force, and also with a zero Lorentz

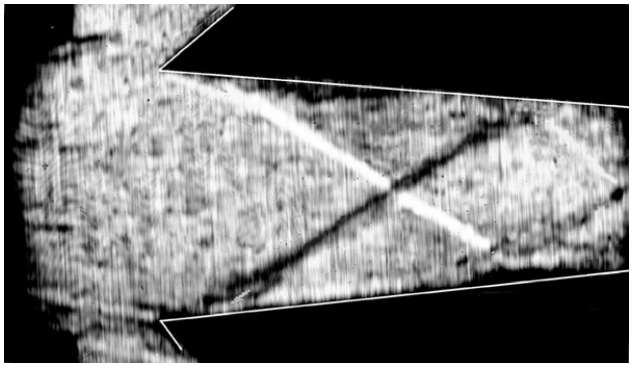

a) V = 125 V, B = −1.3 T, deceleration regime

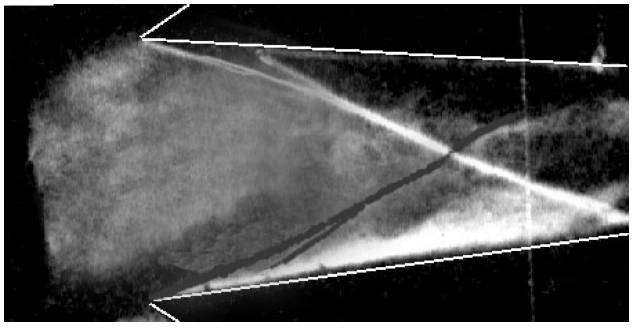

b) V = −150 V, B = −1.3 T, acceleration regime

Fig. 9 Examples of variations in shock-wave configurations under the action of electric and magnetic fields.

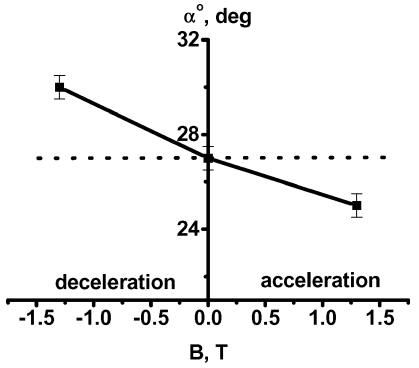

Fig. 10 Variation in interaction angle α of attached shocks.

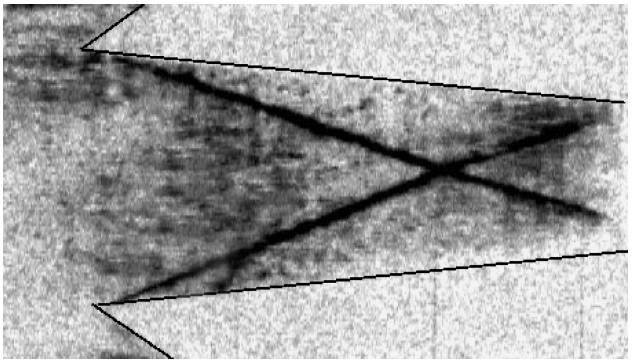

a)

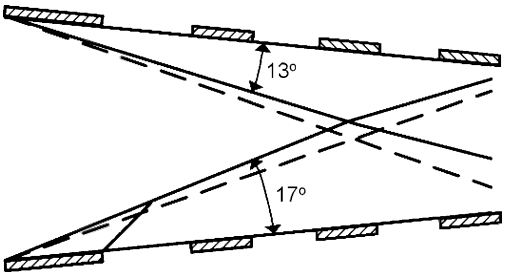

b)

Fig. 11 a) Experiment with longitudinal current: Schlieren picture of the flow and b) the scheme comparing positions of attached shocks.

force. In this series of experiments, the interaction with magnetic and electric fields was localized in the short leading-edge portion of the diffuser, that is, in the region where the action of the fields is most efficient.

Figures 9a and 9b show schlieren pictures of the flow in two cases. Figure 9a presents a schlieren picture for the case when the flow is affected by magnetic and external electric fields in the MHD deceleration regime (Fig. 2a) for $V = 125$ V and $B = -1.3$ T. It can be seen that the combined action of magnetic and electric fields leads to a more considerable flow deceleration, that is, an increase in angle α and decrease in distance x_c. Figure 9b shows a schlieren picture of the flow in the acceleration regime (Fig. 2b) for $V = -150$ V and $B = -1.3$ T. Compared with the picture for $V = 0$, $B = 0$ (Fig. 5a), the angle α is larger, and the distance x_c is smaller, that is, no flow acceleration is observed. This is likely to be because the deceleration caused by Joule heating prevails over the acceleration caused by the Lorentz force. However, comparison of Figs. 9a and 9b shows that the deceleration effect caused by Joule heating can be weakened if an accelerating Lorentz force exists.

It is possible to separate the MHD action from the action of electric field by tracing changes in any characteristic parameter of the shock-wave configuration, for instance, changes in angle α with respect to the angle α in the shock-wave configuration arising under the action of the electric field alone (Fig. 8a). In processing the data, we assumed that change-over from the deceleration to the acceleration regime results from the change in the magnetic induction. The dependence of angle α on magnetic induction is presented in Fig. 10. The horizontal line shows that $\alpha = 27$ deg at $B = 0$. It is evident from Fig. 10 that, as expected, the angle α increases relative to this value in the deceleration regime and decreases in the acceleration regime.

Experiments with Longitudinal Current

Experiments with Longitudinal Current Localized in a Narrow near-Wall Region

The experiment is shown schematically in Fig. 4a. The current is circulated through the third and fourth electrodes and flows in a narrow near-wall region. The values of the current passing through the upper and lower electrodes are 40 and 500 A, respectively. The magnetic field induction is $B = -1.3$ T. Figure 11a shows a shot of the flow. First of all, attention is paid to the asymmetric positions of attached shocks. For illustrative purposes, Fig. 11b also presents positions of shocks in the absence of external fields (dashed lines) and the scheme of positions of shocks in the shot (solid lines). At $B = 0$ and $V = 0$ the shocks are symmetric relative to the axis; the angle between the shock and diffuser wall is $\varphi = 15$ deg. When magnetic and electric fields are applied, the angle of inclination of the shock near the upper wall decreases, while the angle of inclination of the shock near the lower wall increases. This behavior of attached shocks can be explained by the fact that the upper shock moves closer to the upper wall because the gas pressure decreases as a result of the directed action of the Lorentz force. Near the lower wall, the Lorentz force acts in the opposite direction and leads to a pressure increase, and, as a consequence, the shock moves further from the wall. It is useful to compare the flow picture shown in Fig. 11a with the results of the experiment with the transverse current and interaction at the diffuser inlet (commutation regime III, Fig. 8). In both cases, the values of the current through electrodes, the magnetic fields, and interaction zone lengths are nearly equal.

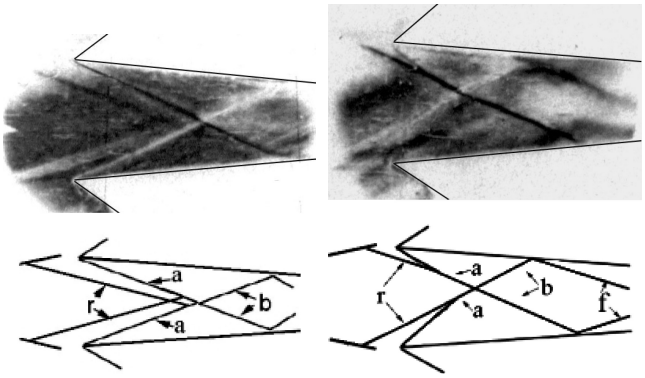

a) $V = -150$ V, $B = 0$ T **b) $V = -150$ V, $B = -1.3$ T**

Fig. 12 Schlieren pictures and schemes of shock-wave configurations. The symbols in the scheme denote basic gasdynamic discontinuities: a, attached shocks; b, the shocks resulting from interaction of attached shocks, f, the shocks reflected from the diffuser walls, and r, the shocks formed near the nozzle electrodes caused by heating of the near-wall layer.

This implies that the energy expenditures in these two cases are nearly the same. However, the near-wall current localization causes smaller changes in the positions of attached shocks, that is, this method is less efficient. The advantage of this method is that it does not cause considerable changes in the flow core.

Experiments with the Longitudinal Current in the Entire Diffuser Volume

In the experiment, a voltage $V = -150$ V was applied to the second and fifth electrodes on the upper and lower nozzle and diffuser walls. The second pair of electrodes on the upper and lower wall of nozzle served as cathodes, and the fifth pair of electrodes in the diffuser were the anodes. Figure 12 presents schlieren pictures of the flow for the cases when only the electric field is applied (Fig. 12a) and when both the magnetic and electric fields are applied simultaneously (Fig. 12b). The average current was 600 A. At such large currents the gas heating is extremely intense near the electrodes. Evidently, this gave rise to the oblique shocks on the near-wall layers in the aft end of the nozzle.[4,15] These shocks are denoted by r in Figs. 12a and 12b. These shocks complicate the picture and make the interpretation of the shock-wave configuration in the diffuser more difficult and ambiguous.

In the absence of magnetic field (Fig. 12a), the flow pattern is symmetric. When the external magnetic field is applied, the pattern becomes asymmetric, as shown in Fig. 12b. The asymmetry of the shock-wave configuration can be explained by the fact that the Lorentz force is directed so that the gas pressure increases near the lower wall, and, as a result, the inclination angle of the attached shock increases. Near the lower wall, the pressure decreases, and the attached shock moves closer to the wall. Comparing the flow pictures in the absence (Fig. 12a) and presence of magnetic field (Fig. 12b), in this case the force effect of the magnetic field turns out to be more appreciable than for other ways of current commutation.

Conclusions

The possibility of controlling attached shocks in a diffuser in the case of both transverse and longitudinal current flows has been demonstrated. It has been found that in the case of the transverse current flow, the Lorentz force causes deceleration (acceleration) of the flow, and in the case of the longitudinal current flow it causes compression (expansion) of the gas volume. A method for separating the action of the Lorentz force from the combined action of external magnetic and electric fields has been developed. It has been shown that to change positions of attached shocks, it is more energetically efficient to apply external fields near the inlet leading edge.

Acknowledgments

The authors wish to gratefully acknowledge support of this work by the European Office of Aerospace Research and Development (ISTC Contract 2009).

References

[1]Gurijanov, E. P., and Harsha, P. T., "AJAX: New Direction in Hypersonic Technology," *7th International Space Planes and Hypersonic Systems and Technologies Conference*, Norfolk, VA, 8–22 Nov. 1996.

[2]Fraishtadt, V. L., Kuranov, A. L., and Sheikin, E. G., "Use of MHD Systems in Hypersonic Aircraft," *Technical Physics*, Vol. 43, No. 11, 1998, pp. 1309–1313.

[3]Bityurin, V. A., Lineberry, J. T., Potebnia, V. G., Alferov, V. I., Kuranov, A. L., and Sheikin, E. G., "Assessment of Hypersonic MHD Concepts," *28th Plasmadynamics and Lasers Conference*, Atlanta, 23–25 June 1997.

[4]Brichkin, D. I., Kuranov, A. L., and Sheikin, E. G., "MHD-Technology for Scramjet Control," *8th AIAA International Space Planes and Hypersonic Systems and Technologies Conference*, Norfolk, VA, 27–30 April 1998.

[5]Golovachov, Yu. P., and Suschikh, S. Yu., "Supersonic Air-Scoop Flows of a Weakly Ionized Gas in External Electromagnetic Field," *Technical Physics*, Vol. 45, No. 2, 2000, pp. 168–173.

[6]Vatazhin, A., Kopchenov, V., and Gouskov, O., "Numerical Investigation of Hypersonic Inlets Control by Magnetic Field," IVTAN, April 2000.

[7]Macheret, S. O., Shneider, M. N., and Miles, R. B., "Modelling of Air Plasma Generation by Electron Beams and High-Voltage Pulses," *31st AIAA Plasmadynamics and Lasers Conference*, Denver, CO, 19–22 June 2000.

[8]Golovachov, Yu. P., Sushchikh, S. Yu., and Van Wie, D. M., "Numerical Simulation of MGD Flows in Supersonic Inlets," *31st AIAA Plasmadynamics and Lasers Conference*, Denver, CO, 19–22 June 2000.

[9]Golovachov, Yu. P., Kurakin, Yu. A., Schmidt, A. A., and Van Wie, D. M., "Numerical Investigation of Non-Equilibrium MGD Flows in Supersonic Intakes," *32nd AIAA Plasmadynamics and Lasers Conference, and 4th Weakly Ionized Gases Workshop*, Anaheim, CA, 11–14 June 2001.

[10]Bobashev, S. V., Golovachov, Yu. P., and Van Wie, D. M., "Deceleration of Supersonic Plasma Flow by Applied Magnetic Field," *33rd Plasmadynamics and Lasers Conference*, Maui, Hawaii, 20–23 May 2002.

[11]Bobashev, S. V., D'yakonova, E. A., Erofeev, A. V., Lapushkina, T. A., Sakharov, V. A., Vasil'eva, R. V., and Van Wie, D. M., "MHD Design Features in Supersonic Single-Shock Diffuser," *Proceedings of International Conference on MHD Power Generation and High Temperature Technologies 1999*, Vol. II, 1999, pp. 581–587.

[12]Bobashev, S. V., Vasil'eva, R. V., D'yakonova, E. A., Erofeev, A. V., Lapushkina, T. A., Maslennikov, V. G., Poniaev, S. A., Sakharov, V. A., and Van Wie, D., "The Effect of MHD Interactions on the Input Shock Waves in a Supersonic Diffuser," *Technical Physics Letters*, Vol. 27, No. 1, 2001, pp. 71–73.

[13]Bobashev, S. V., D'yakonova, E. A., Erofeev, A. V., Lapushkina, T. A., Maslennikov, V. G., Poniaev, S. A., Sakharov, V. A., Vasil'eva, R. V., and Van Wie, D. M., "Shock-Tube Facility for MGD Supersonic Flow Control," *21st AIAA Aerodynamic Measurement Technology and Ground Testing Conference*, Denver, CO, 19–22 June 2000.

[14]Bobashev, S. V., Erofeev, A. V., Lapushkina, T. A., Poniaev, S. A., Sakharov, V. A., Vasil'eva, R. V., and Van Wie, D., "Strong Action of Magnetic and Electrical Fields on Inlet Shock Configuration in Diffuser," *4th Workshop on Magnetoplasma Aerodynamics for Aerospace Application*, IVTAN, April 2002.

[15]Lapushkina, T. A., Bobashev, S. V., Vasil'eva, R. V., Erofeev, A. V., Poniaev, S. A., and Sakharov, V. A., "Influence of Electric and Magnetic Fields on Shock-Wave Configuration in Diffuser," *Technical physics*, Vol. 47, No. 4, 2002, pp. 397–405.

[16]Bobashev, S. V., Erofeev, A. V., Lapushkina, T. A., Poniaev, S. A., Sakharov, V. A., Vasil'eva, R. V., and Van Wie, D. M., "Effect of the Wall Layers on the Electric Current in a Model of MHD Diffuser," *32nd AIAA Plasmadynamics and Lasers Conference, and 4th Weakly Ionized Gases Workshop*, Anaheim, CA, 11–14 June 2001.

[17]Bobashev, S. V., Erofeev, A. V., Lapushkina, T. A., Poniaev, S. A., Vasil'eva, R. V., and Van Wie, D. M., "Experiments on MHD Control of Attached Shocks in Diffuser," *41st Aerospace Science Meeting and Exhibit*, Reno, NV, 6–9 Jan. 2003.

[18]Biberman, L. M., Vorob'ev, L. H., and Yakubov, V. S., *Kinetics of the Non-Equilibrium Low-Temperature Plasma*, Nauka, Moscow, 1962, p. 376 (in Russian).

[19]Raizer, Yu. P., *Gas Discharge Physics*, Springer-Verlag, Berlin, 1991.

[20]Vasil'eva, R. V., D'yakonova, E. A., Erofeev, A. V., and Lapushkina, T. A., "Development of Ionization in Noequilibrium Inert Gas Plasmas in Magnetogasdynamics Channel," *Technical Physics*, Vol. 44, No. 11, 1999, pp. 1312–1317.

[21]Vasil'eva, R. V., Genkin, A. L., Goryachev, V. L., Erofeev, A. V., Zuev, A. D., Mironov, D. N., Remennyi, A. S., and Silin, N. A., *Low-Temperature Plasma of Inert Gases with Non-Equilibrium Ionization and MHD Generators*, Physico-Technical Inst., Russian Academy of Sciences, St. Petersburg, 1991, pp. 1–206 (in Russian).

[22]Vulis, L. A., Genkin, A. L., and Fomenko, B. A., *Theory and Calculation of Magnetogasdynamic Flows in the Channels*, Atomizdat, Moscow, p. 384, 1971 (in Russian).